

## Appendix C: SCAPE Modelling of Shore Evolution: Cromer to Cart Gap

Mott MacDonald

08 August 2013

Final Report

9W6431



Stratus House  
Emperor Way  
Exeter, Devon EX1 3QS  
United Kingdom  
+44 1392 447999

info@exeter.royalhaskoning.com  
www.royalhaskoningdhv.com

Telephone  
Fax  
E-mail  
Internet

Document title	Appendix C: SCAPE Modelling of Shore Evolution: Cromer to Cart Gap
Document short title	
Status	Final Report
Date	08 August 2013
Project name	Cromer to Winterton Ness Coastal Study
Project number	9W6431
Client	Mott MacDonald
Reference	9W6431/R/303948/Exet

Drafted by	Mike Walkden
Checked by	Rachel Bird
Date/initials check	.....
Approved by	Pippa Lawton
Date/initials approval	.....



## CONTENTS

	Page
1 INTRODUCTION	1
2 THE CLIFFS AND SHORE	2
2.1 Representation of hydrodynamic conditions	4
3 THE MODEL	5
3.1 Cliff slope failure	7
3.2 Discretisation of the coast	8
3.3 Model validation	8
4 SIMULATIONS	10
4.1 Climate Change Projections	10
4.2 Management Scenarios	10
4.3 Probabilistic application	11
5 RESULTS	12
6 INTERPRETATION	21
6.1 Recession at Trimmingham	21
6.2 Recession at Overstrand	24
7 SUMMARY	32



## 1 INTRODUCTION

Royal HaskoningDHV was commissioned by Mott MacDonald to run a numerical geomorphological model of the shore of North Norfolk (UK) between Cromer and Cart Gap. This work is an element of the Cromer to Winterton Ness Coastal Study, which Mott MacDonald is undertaking for North Norfolk District Council.

The modelling work used the Norfolk model initially built by the University of Bristol for the Overstrand to Walcott Strategy Study (University of Bristol, 2002, Walkden and Hall 2011), and later extended and refined by Newcastle University and the Tyndall Centre for Climate Change Research (Dickson *et al*, 2007, Dawson *et al*, 2009). Consequently this study did not require or include model construction, calibration or validation. The Norfolk model was constructed using the modelling tool Soft Cliff And Platform Erosion (SCAPE, see Walkden and Hall, 2005), and it was run probabilistically, to account for a set of inherent uncertainties.

The model was used to explore geomorphic response to two alternative scenarios of coastal management: named 'Do Nothing' (or Scenario 1) and 'SMP Policy 6' (or Scenario 2). This was achieved in the model by representing the loss or removal of coast protection structures, where this would occur as a consequence of the management policy.

The outputs for each management policy were: (1) annual projections of cliff top recession distance and (2) annual southerly beach sediment flux at Cart Gap. These were then used by Mott MacDonald to assess the relative merits of the management policies.

This report provides an overview of the cliffs within the study area and the sedimentary system fronting them. The modelling tool SCAPE is then outlined, and the development of the specific model used in this study is described. The treatment of the two management scenarios is then described, as is the representation of climate change and the probabilistic approach to the simulations. The results of the study are then presented, with some exploration of the importance of the exchange of sediment between neighbouring sections of the model.

Further to the work included in this report, relating to management Scenarios 1 and 2, a subsequent investigation into further two Scenarios (3 and 4) has been carried out. Scenario 3 is a modified version of Scenario 2 (SMP2 Policy 6), where a hold the line has been taken at Overstrand, Mundesley, Bacton, Walcott and Ostend over the long term. Scenario 4 (SMP2 Policy 6, with additional sediment nourishment) is identical to Scenario 2 with the addition of extra beach nourishment from Trimingham to Overstrand. The Addendum to this report describes the investigations into management Scenarios 3 and 4 and the findings.

## 2 THE CLIFFS AND SHORE

The coast of northeast Norfolk (see Figure 1 and Figure 6) features an almost continuous line of cliffs between Weybourne in the north, where cliffs are composed of relatively resistant chalk overlain by glacial-tills, and Happisburgh/Eccles in the south, where they are composed of less resistant glacial-tills. The transition from predominantly chalk to till in the cliff-toe occurs between Weybourne and Cromer, and roughly coincides with the location of a well-documented divide in the direction of longshore sediment transport (Vincent 1979; Clayton 1989; Chang and Evans 1992). Due to the drift divide the direction of sediment transport is mainly southeast from around Cromer. The potential for transport tends to build with distance south as the coastline curves.

The average height of the cliffs is approximately 20 metres, but they reach a maximum of approximately 60 metres at Trimmingham and to the south of Cromer.

Erosion of soft-cliff slopes occurs largely through processes of mass movement, that result from some combination of critical slope angles and stresses within rock or partially consolidated masses. In this respect erosion is sensitive both to marine processes, which can undercut and steepen cliffs, as well as the interplay between the geotechnical properties of the cliff and subaerial erosion processes (Lee and Clark 2002). However, the primary controls on long term rates of cliff retreat are the gradient and elevation (relative to sea level) of the shore platform and beach, as these control the ability of waves to clear fallen debris and then attack and destabilise the cliff toe.

Evolution of this coastline over the last 150 years has been increasingly influenced by the construction of seawalls, groynes, and palisades, mostly between 1950 and 1980, protecting considerable stretches of the coast. This construction began at Mundesley where a groyne was constructed in 1860, followed by a seawall in 1880. Groynes were constructed in Cromer in 1875 and at Overstrand in 1890. Seawalls were built at both Cromer and Sheringham in 1875. This history is illustrated graphically in Figure 1.



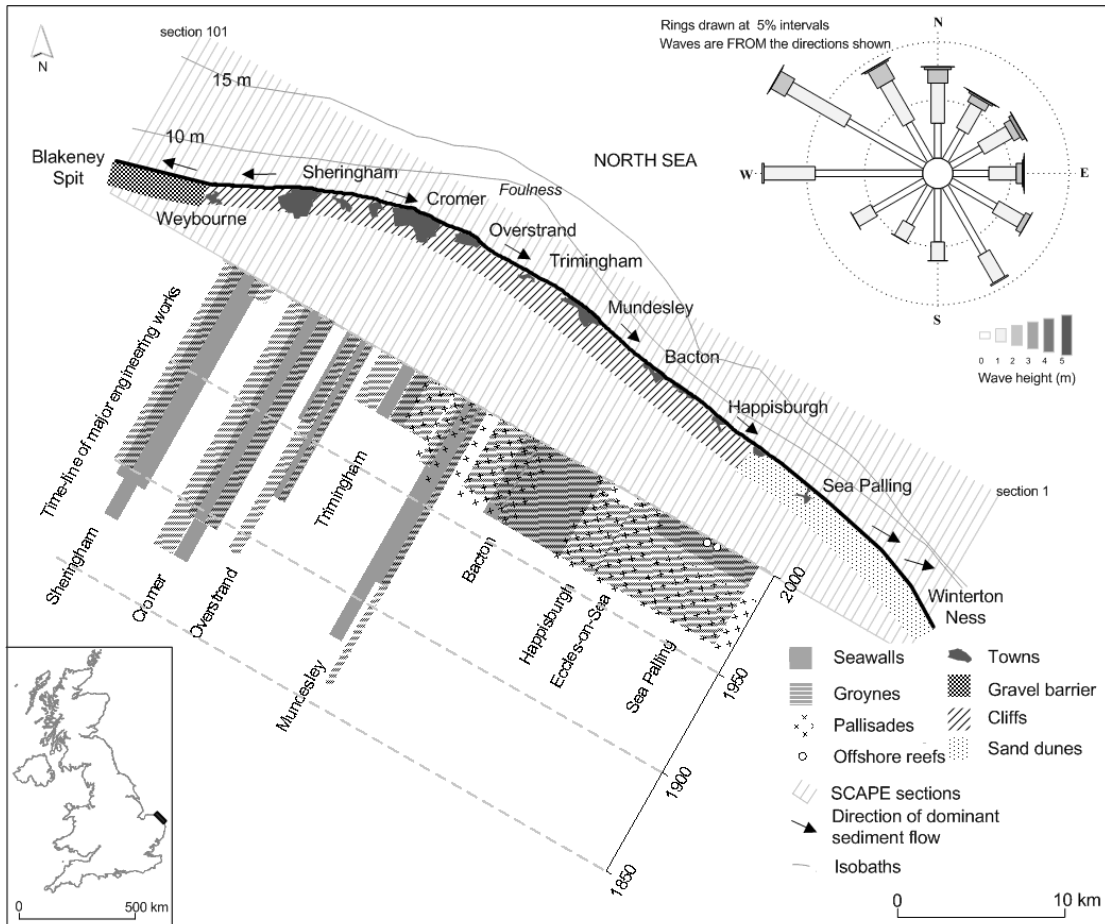


**Figure 1. History of coastal interventions along the cliffs of North Norfolk (Modified from Dickson et al, 2007); note that (in the wave rose in this figure) wave height is indicated by bar width and shading, and bar length indicates the proportion of all waves arriving from the shown direction.**

This engineering intervention has resulted in the protrusion of settlements seaward of the general line of the coast, as adjacent unprotected areas have continued to recede. Sheringham, Cromer, Overstrand, and Mundesley protrude by approximately 120 metres, 150 metres, 220 metres, and 150 metres, respectively, and each of these artificial headlands is a few kilometres wide.



**Figure 2.** ‘Artificial’ protrusion of the settlements of Cromer and Overstrand from the ‘natural’ alignment of the coast (image copyright Google).

## 2.1 Representation of hydrodynamic conditions

This region of coast is exposed to waves generated within the North Sea. For wave directions between approximately 0 degrees and 70 degrees the fetch lengths are greater than 500 kilometres, and it is from these directions that the largest waves arrive (as illustrated in the wave rose within Figure 1).

To create an appropriate input to the numerical model, wave heights, periods, and directions at the site were hindcast from a wind record that was collected between 1978 and 1994 at Gorleston, near Great Yarmouth. This record was modified to represent offshore conditions and extended to 2001 using weather model data (University of Bristol, 2002). This was used to hindcast offshore waves at Ordnance Survey national grid reference 636836E, 350606N, which is approximately 13 km offshore of the middle of the model. The influence of Haisborough Sands, a large local sandbank, was represented by limiting the maximum wave height.

High-tide levels are also required for the model and these were extracted from a 13-year record of tide levels at Cromer. This location is towards the northern end of the model, so the data were transformed to represent conditions at Mundesley, which is more central. This transformation was based on linear interpolation between tidal characteristics at Cromer and Lowestoft.

### 3 THE MODEL

The original Norfolk model was built using the SCAPE modelling tool (Walkden and Hall, 2005) for the Overstrand to Walcott Strategy study (North Norfolk, 2004). It was then developed, over a period of four years, with funding from the Tyndall Centre for Climate Change research (Walkden and Hall, 2011, Dickson *et al*, 2007). The model formed the central geomorphic engine of the Regional Coastal Simulator of the Tyndall Centre for Climate Change Research, as described by Dawson *et al*, 2009. The work has been well received, and was, for example, the recipient of the Lloyds Science in Risk Prize in 2012.

SCAPE represents a number of processes and their interactions including:

- Wave transformation from the nearshore points (provided by a TOMAWAC model, see Dawson *et al*, 2009) to the breaker point using linear wave theory.
- Sediment exchange between the beach and a nearshore bar using a simple parameterization of the COSMOS model (Nairn and Southgate 1993).
- Longshore sediment transport using a one-line beach model (Pelnaud-Considerere 1956) of the form described in Hanson (1989).
- Erosion of the shore platform and cliff toe (Walkden and Hall 2005).
- Delivery of talus to the beach.
- The effect of shore parallel coastal structures (seawalls and palisades) and groynes as follows: (1) seawalls prevent cliff toe retreat, but do not stop lowering, of the shore platform, (2) palisades reduce the heights of passing waves by 50%, and (3) groynes reduce longshore sediment transport, except when beaches are wider than the structures.

Figure 3 illustrates the way the shore profile is conceptualised within the model and the integration of erosive potential for a single tidal timestep. At every stage of the tidal oscillation the breaking wave field has the potential to erode the rock surface. This is represented by a function  $f_1$ . The seaward extent of  $f_1$  is approximately equal to the water depth at which waves begin to break. To obtain the total erosive potential over a tidal cycle the instantaneous distribution of erosion must be integrated over the tidal period.

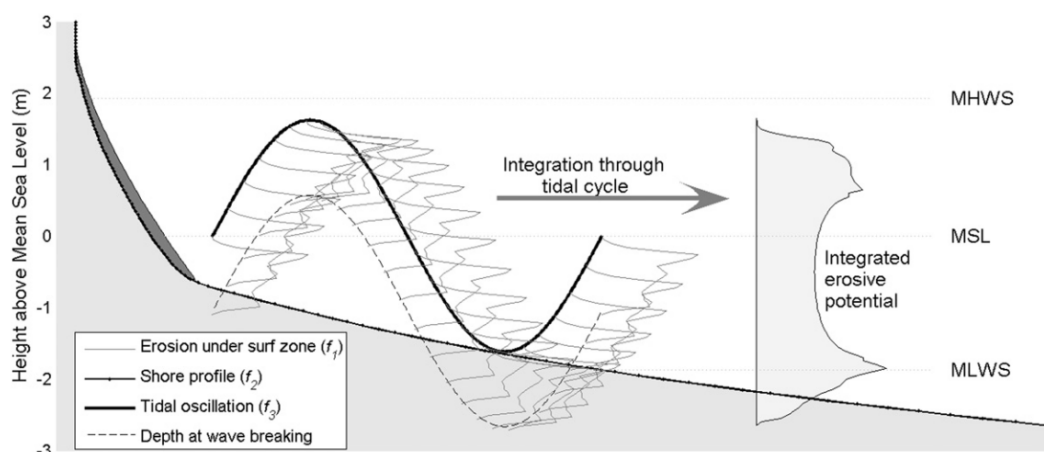


**Figure 3. Conceptualisation of the shore profile (from Walkden and Dickson, 2008)**

As can be seen in Figure 3 the integrated erosive potential tends to be concentrated at the tidal extremes, simply because this is where the water level spends the most time. Importantly, the actual erosion experienced by any exposed rock element also depends on (the tangent of) its slope. This means that gently sloping elements (generally lower in the profile) tend to erode less than the (typically higher) steeper elements.

In more formal terms, every timestep erosion of each element ( $\Delta y$ ) is calculated with the expression:

$$\frac{\Delta y}{\Delta t} = H_b^{13/4} T^{3/2} K^{-1} f_1(f_3(t) - z) \tan(f_2(z)) \quad \text{Equation 1}$$

Where horizontal and vertical dimensions are  $y$  and  $z$  respectively,  $t$  is time,  $H_b$  is the breaking wave height,  $T$  is the wave period and  $K$  is a calibration term representing rock strength and some hydrodynamic constants, (units  $m^{9/4} s^{2/3}$ ), (see Kamphuis, 1987 and Walkden and Hall, 2005).  $f_1$  is a dimensionless distribution of soft rock erosion under a breaking wave field, which was referred to above and was derived by Walkden and Hall (2005) from physical model tests of Skafel (1995).  $f_2$  is the tidal variation in water level, which is represented as a sinusoid about mean sea level (MSL).  $f_3$  is the slope of each rock element and therefore changes throughout the simulation in response to the calculated erosion. Gradually the model iterates towards a profile form that is in dynamic equilibrium with the input conditions. Sea level rise is implemented as a shifting frame of reference.

A particular strength of the Norfolk model is its regional coverage, and its representation of interactions between: (1) different elements of the coastal system (cliff, beach, platform, hydrodynamics) and (2) neighbouring sections of coasts. Some of these interactions are illustrated in the 'system map' provided as Figure 4.

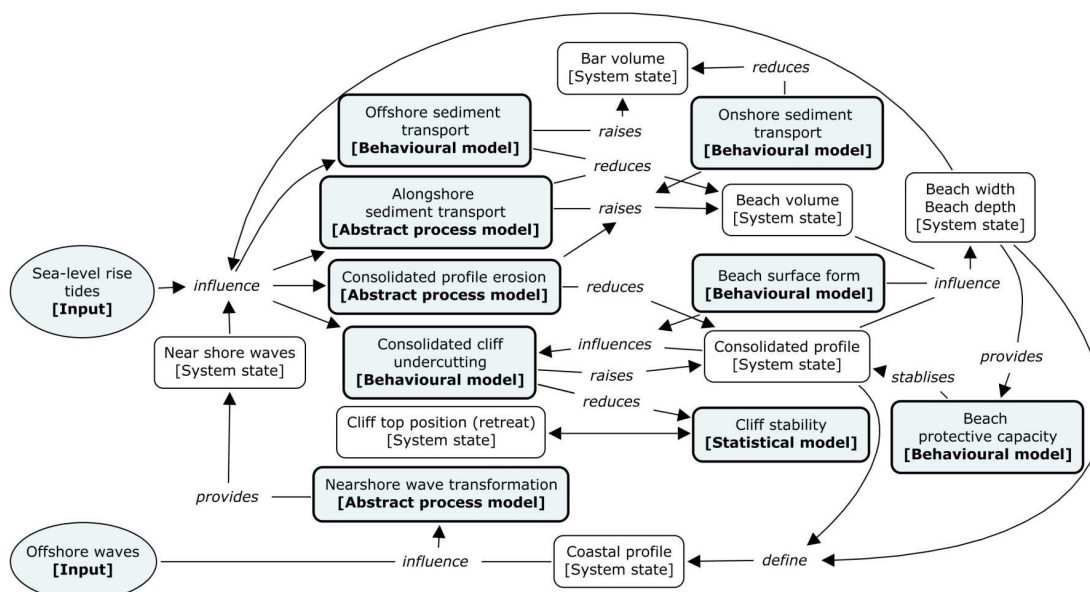


**Figure 4. 'Systems map' of interactions within SCAPE**

### 3.1 Cliff slope failure

The SCAPE simulations predict (amongst other things) the position of the cliff toe. For economic appraisal, predictions are required of when individual cliff-top assets will be lost due to cliff failure.

Coastal cliff land-sliding occurs as a consequence of both cliff toe recession and geotechnical processes within the cliff slope. Land-sliding of these cliffs is preceded by marine removal of material from the cliff toe, resulting in coastal slope steepening. Eventually a landslide occurs that delivers debris to the beach and reduces the coastal slope. The time at which this occurs depends on the rate of material removal and geotechnical processes, and cannot be predicted precisely. However, the rate of shoreline retreat from SCAPE can be combined with a geotechnical assessment to generate an approximate probability distribution of the possible cliff top location after failure (Hall *et al.* 2000). The approach used here is based on the concept of a Cliff Behavioural Unit (CBU), which is a frontage of cliff-line which behaves in a broadly uniform way. Within a CBU, the cliff face may be expected to fail when it is steepened to an average angle  $\alpha_f$  and will fail to an angle  $\alpha_s$ . Neither  $\alpha_f$  nor  $\alpha_s$  can be known precisely, but will vary with local variations in cliff strength and composition and temporal variations in pore pressure. This uncertainty has been included in the analysis by representing in  $\alpha_f$  and  $\alpha_s$  as Normally-distributed random variables, with means and variances obtained from a geomorphological assessment of each CBU. This is illustrated diagrammatically in Figure 5.

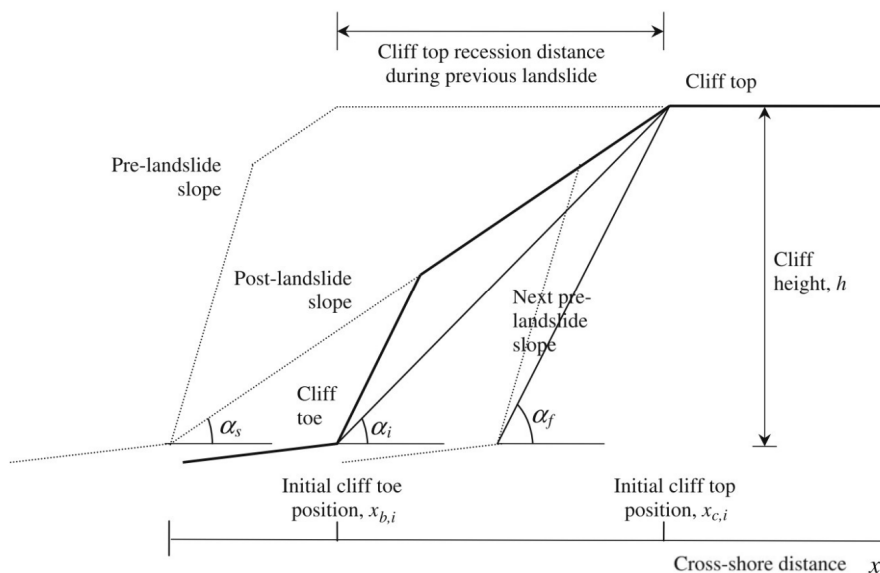


**Figure 5. Coastal landsliding model (Modified from Dawson *et al.*, 2009).**

The initial cliff angle is also represented as a Normally-distributed random variable, with mean and variance based on observations within each CBU. Further details of how the parameters were derived and the model run can be found in Dawson *et al.*, 2009.

### 3.2 Discretisation of the coast

The coast is represented in segments of 500 metres length. Within each segment the shore profile, beach volume and wave conditions are assumed to be constant. The model (including boundary regions) extended 50 kilometres, between the depositional features of Winterton Ness and Blakeney Spit. The centre of each of the 101 model sections is shown in Figure 6.

This discretisation also applies to the representation of the structures, i.e. each section of seawall, revetment, groyne or reef was assumed to extend over a full 500 metre segment. This process of discretisation results in model segments that do not conform precisely to the extents of real structures or management units. A stage of expert assessment is therefore necessary to interpret ‘real life’ consequences of the (discretised) model output.

Such discretisation imposes a limit on the scale at which the model can be expected to provide realistic results. For example the current change in shore alignment at Happisburgh, where the coast steps back by more than 100 metres in a length less than 50 metres, cannot be represented well.

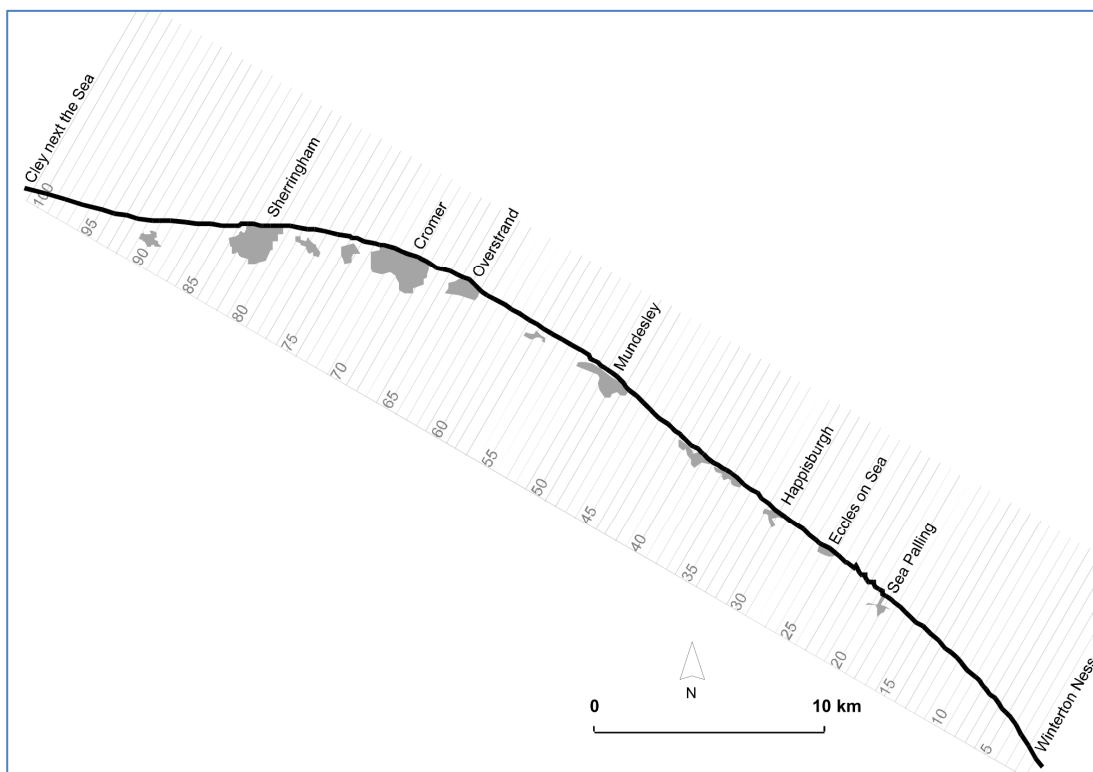


Figure 6. Location of model sections

### 3.3 Model validation

As noted above, the SCAPE model used had already been subject to a detailed process of calibration and validation, and so this was not required in the current study. Details

and results of calibration and validation can be found in both Walkden and Hall, 2011, and in Dickson *et al*, 2007. That process is described, in the outline, below. It should be noted that the process of validation within this study also included close scrutiny of model output by experts with direct local experience.

The shape of the modelled coast, in both profile and plan-view, emerges from the dynamic interaction between, and within, modules, which respond to the imposed loading (chiefly waves, tides and sea level rise) and coastal management interventions. The model contains two calibration terms, coefficients of alongshore transport and rock strength ( $K$  in Equation 1). The transport coefficient was first varied until the general scale of transport along the shore matched perceived rates. The rock strength term was then varied until general recession rates became similar to those observed (see Walkden and Hall, 2011 for a fuller description, and sensitivity testing).

The history of coastal engineering construction was then represented from the later part of the 1800s to 2000, and model behaviour was compared with historical recession data measured from Ordnance Survey maps. Once a satisfactory validation was achieved (see Figure 7, and described fully in Dickson *et al*. 2007), the model was then run to the year 2120 under the climate change and management scenarios required for this study.

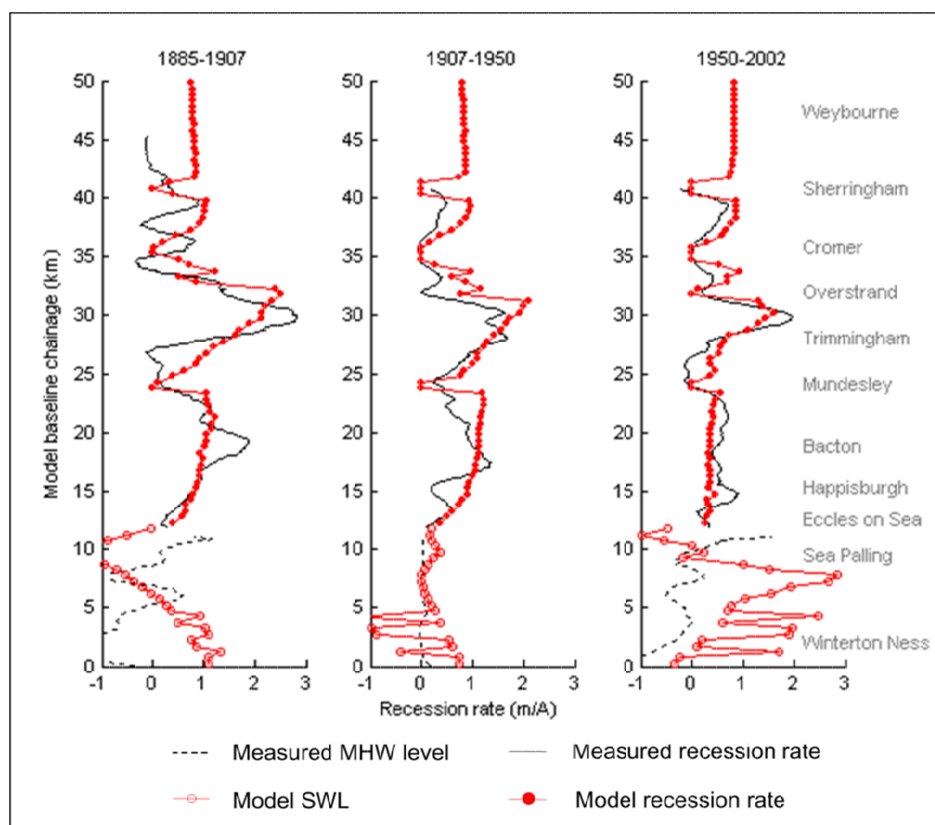


**Figure 7. Comparison of SCAPE model recession rates with those measured from historical maps over three eras, 1885 – 1907, 1907 – 1950 and 1950 – 2002 (Modified from Dickson *et al*, 2007).**

## 4 SIMULATIONS

As part of this study, simulations were run to explore how the cliff top position and sediment flux (from the cliffs towards the south) might vary in response to future management practices and climate change. These simulations extended to the year 2120 and were governed by assumed projections of climate change and scenarios of coastal management.

### 4.1 Climate Change Projections

Climate change was represented in the model through its effects on sea level and wave activity.

Future sea level rise was represented using the 'Upper End Estimate' specified by the Environment Agency (Environment Agency, 2011).

Period	To 2025	2026 to 2050	2051 to 2080	2081 to 2115
Rate of SLR (mm/yr)	4	7	11	15

**Table 1. Assumed rates of sea level rise in mm/yr (Upper End Estimate, From Environment Agency 2011).**

That report (Environment Agency 2011) does not attempt to quantify the effects of climate change on wave conditions, and so previous guidance was followed. The heights of extreme waves were assumed to grow by 5% until the year 2055 and by 10% after that year, as specified in Environment Agency (2006). Wave periods were increased proportionally using Froude Law scaling.

The (highly uncertain) effect of climate change on future wave direction was represented in each simulation by rotating the angle of offshore wave attack by a (normally distributed) random angle of between -10 and + 10 degrees.

### 4.2 Management Scenarios

Two management scenarios were represented, termed 'Do Nothing' (Scenario 1) and 'SMP Policy 6' (Scenario 2). The first of these represented a general policy of not intervening with the future failure of coastal structures, whilst the second represented implementation of the preferred policies of the recent shoreline management plan review (further information on these policies can be found in the report to which this is an appendix). These were implemented by 'switching off' the seawalls, revetments and groynes represented in the model, in particular places at specified years.

The chosen locations and dates of removal/ failure were specified, by Mott MacDonald staff, following inspection of the coast (see Appendix A). The dates were specified as upper and lower estimates of the possible failure year, to represent the inherent uncertainty at the 95% level.



### 4.3 Probabilistic application

The model was run probabilistically in that:

- Each (120 year) Management Scenario was simulated 250 times (i.e. a total of 60,000 years of shore development were run);
- The recession of each Cliff Behavioural Unit was then simulated 50 times per SCAPE simulation (i.e. a total of three million years of cliff development were run);
- Wave and water level sequence were randomly set for each simulation;
- The year of failure of each structure was sampled from a normal distribution (determined by the limits tabulated in Appendix A); and
- The angle of the incident waves was varied randomly, for each simulation, as described above.

The results of this large simulation set were harvested and aggregated into histograms, from which the required outputs were extracted.

## 5 RESULTS

The primary outputs of the simulations were the distance of retreat of the cliff edge relative to their position in 2012. These were extracted from the probabilistic results and provided at the 5% and 95% levels.

The annual average sediment transport rates were also provided where the cliffs meet low-lying land (at Cart Gap, model section 29). These were given at a range of exceedance levels. The results are illustrated in Figure 8 to Figure 15 below.

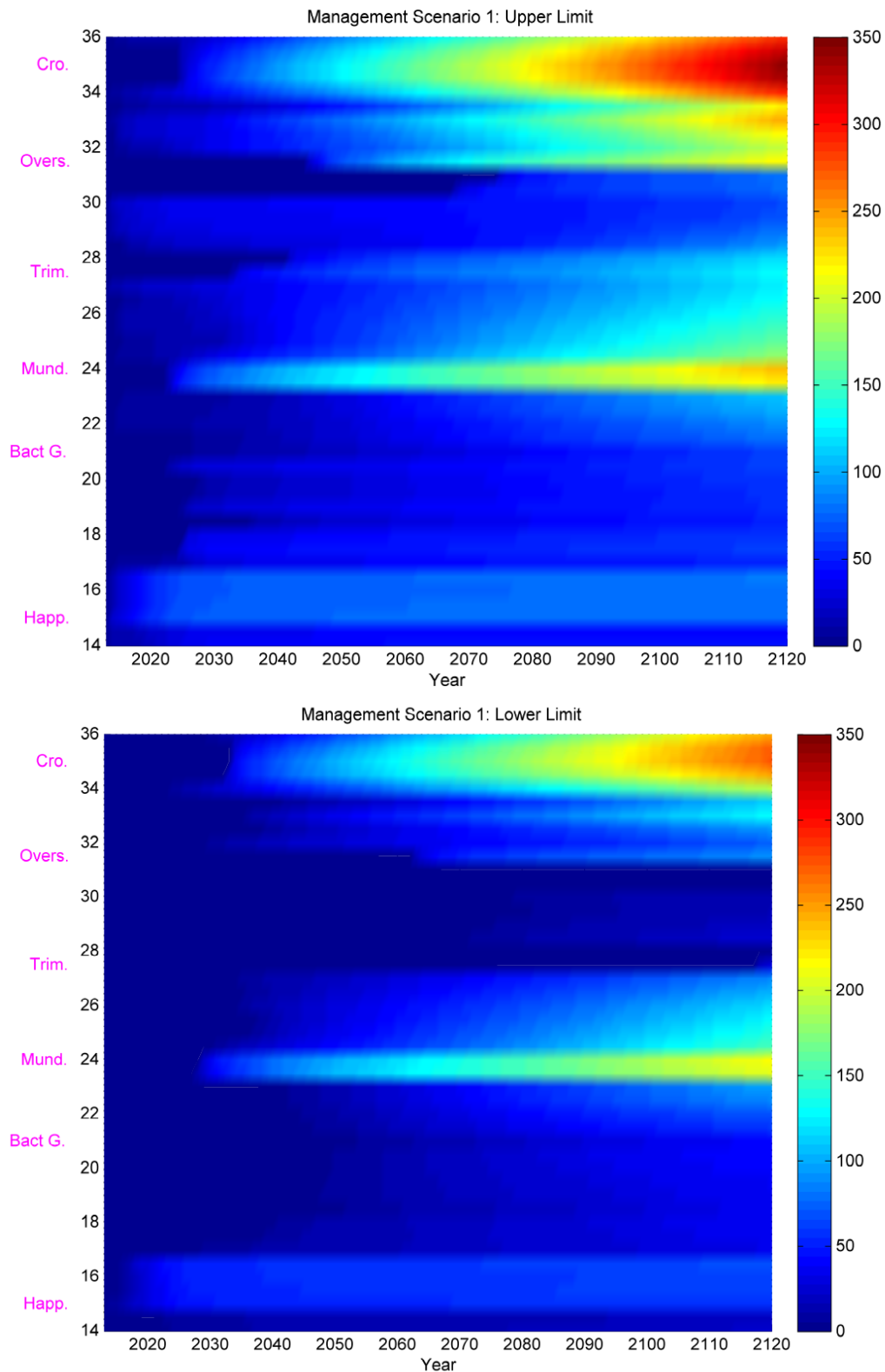
The differences between the upper and lower estimates of recession, for both scenarios, can be seen in Figure 8 and Figure 9. Time is represented by the horizontal axis, whilst the vertical axis represents the position along the coast. Colour represents recession distance, with a scale from 0 (blue) to 350 metres (red). For example, in Figure 8, a horizontal band of colour can be seen at the top of the images, which grades from blue to red (upper estimate of recession rate) and from blue to orange (lower estimate of recession rate). These represent the range of projected erosion at Cromer i.e. the cliff is expected to have receded by between approximately 270 metres and 340 metres by 2120. In contrast, the same part of the upper and lower panels in Figure 9 show a dark blue band, indicating an absence of erosion, due to continued coast protection at Cromer.

In general terms more severe erosion is present in the north of the study area (i.e. around Cromer) under Management Scenario 1 ('Do Nothing'), however, more erosion is evident across the southern half of the study area under Management Scenario 2 ('SMP2 Policy 6'). The reason for this behaviour is discussed below, and the economic consequences of these erosion patterns have been quantified in the main report.

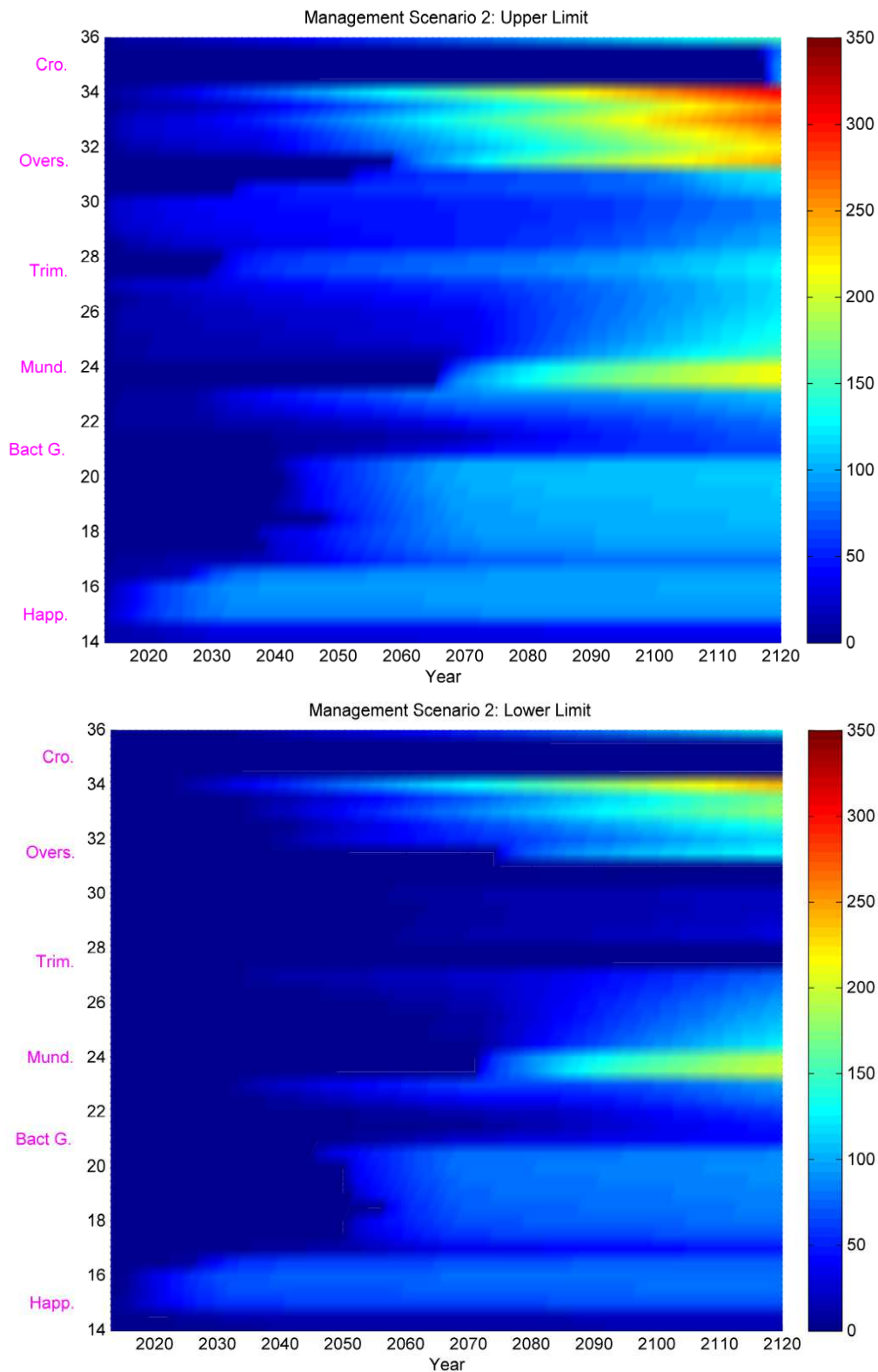
The same information is presented in a different form in Figure 10 to Figure 13. These show cliff toe recession (as possible ranges) for each of the years 2025, 2055, 2085 and 2120, for both management scenarios.

Figure 14 shows the average annual sediment transport rates at Cart Gap, where positive values indicate transport north and negative values indicate transport south. These are shown for various estimates ranging from upper estimates (99%) to lower estimates (1%) (as highlighted by the figures on the right hand side). The upper image shows the results for Management Scenario 1 ('Do Nothing') and the lower image shows the results for the Management Scenario 2 ('SMP2 Policy 6').

Figure 15 then combined the results from the upper (95%), best (50%) and lower (5%) estimates for the two management scenarios for ease of comparison. The results of this are discussed below.



**Figure 8. Cliff top recession distances (in metres) across the study area as a consequence of Management Scenario 1 ('Do Nothing'). The vertical axis represents distance from Winterton Ness, in kilometres. The top image shows the upper estimate of recession whilst the lower image shows the lower estimate.**



**Figure 9. Cliff top recession distances (in metres) across the study area as a consequence of Management Scenario 2, ('SMP2 Policy 6')** The vertical axis represents distance from Winterton Ness, in kilometres. The top image shows the upper estimates of recession whilst the lower image shows the lower estimate.

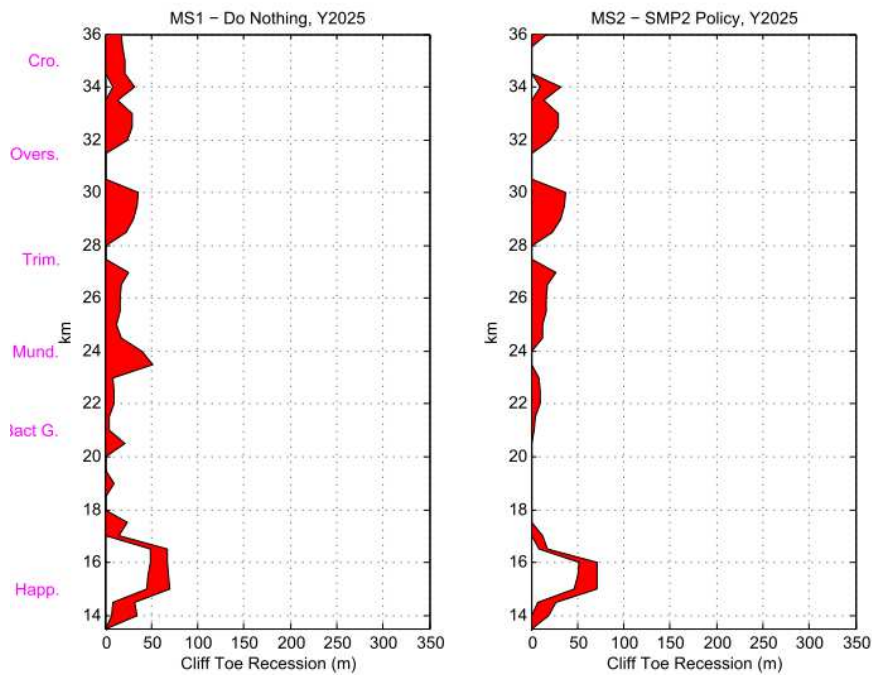


**Figure 10. Cliff top recession (as a range) for year 2025; note that the vertical axis represents distance from Winterton Ness (in kilometers), and that the position of various settlements is indicated on the left hand side.**

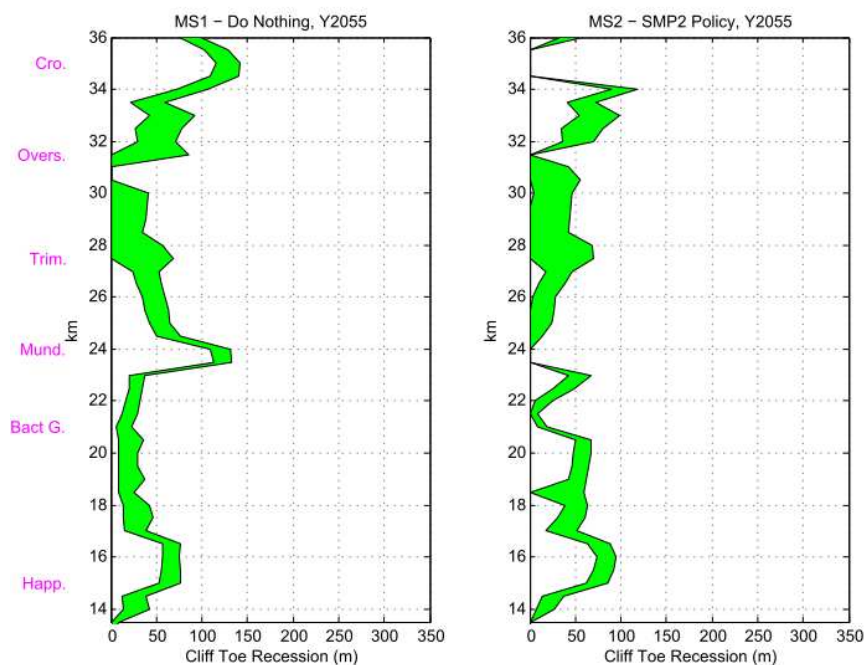


**Figure 11. Cliff top recession (as a range) for year 2055; note that the vertical axis represents distance from Winterton Ness (in kilometers), and that the position of various settlements is indicated on the left hand side.**

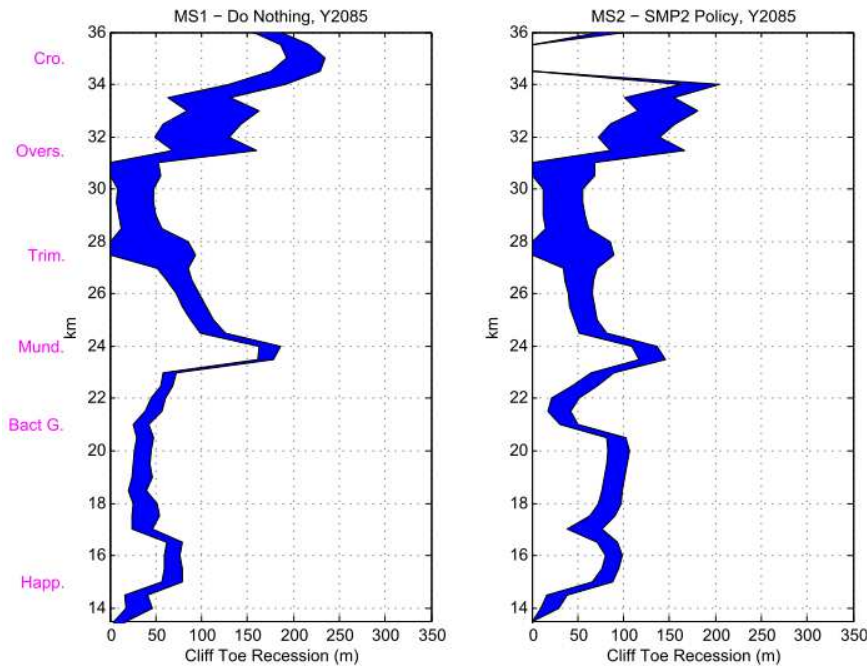


Figure 12. Cliff top recession (as a range) for year 2085; note that the vertical axis represents distance from Winterton Ness (in kilometers), and that the position of various settlements is indicated on the left hand side.

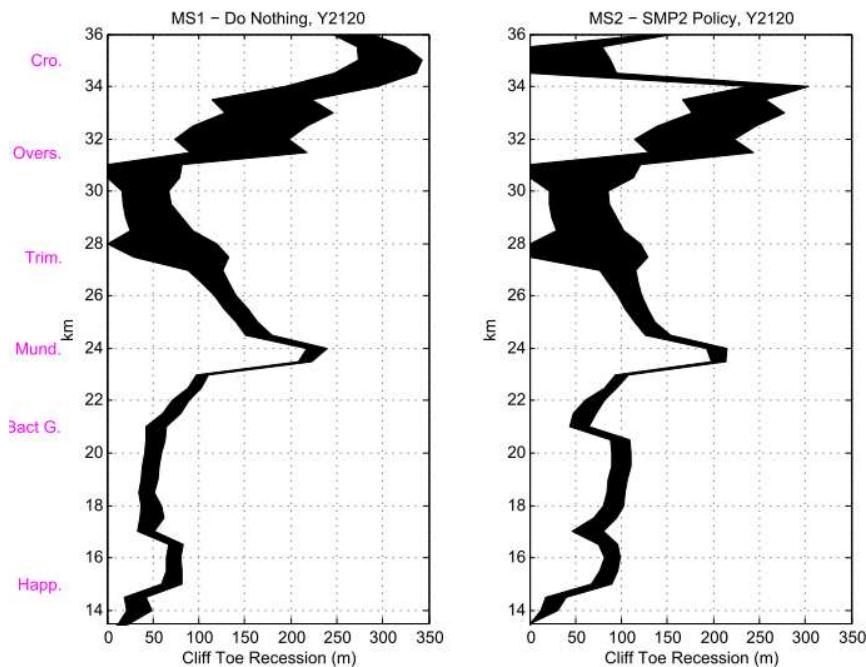
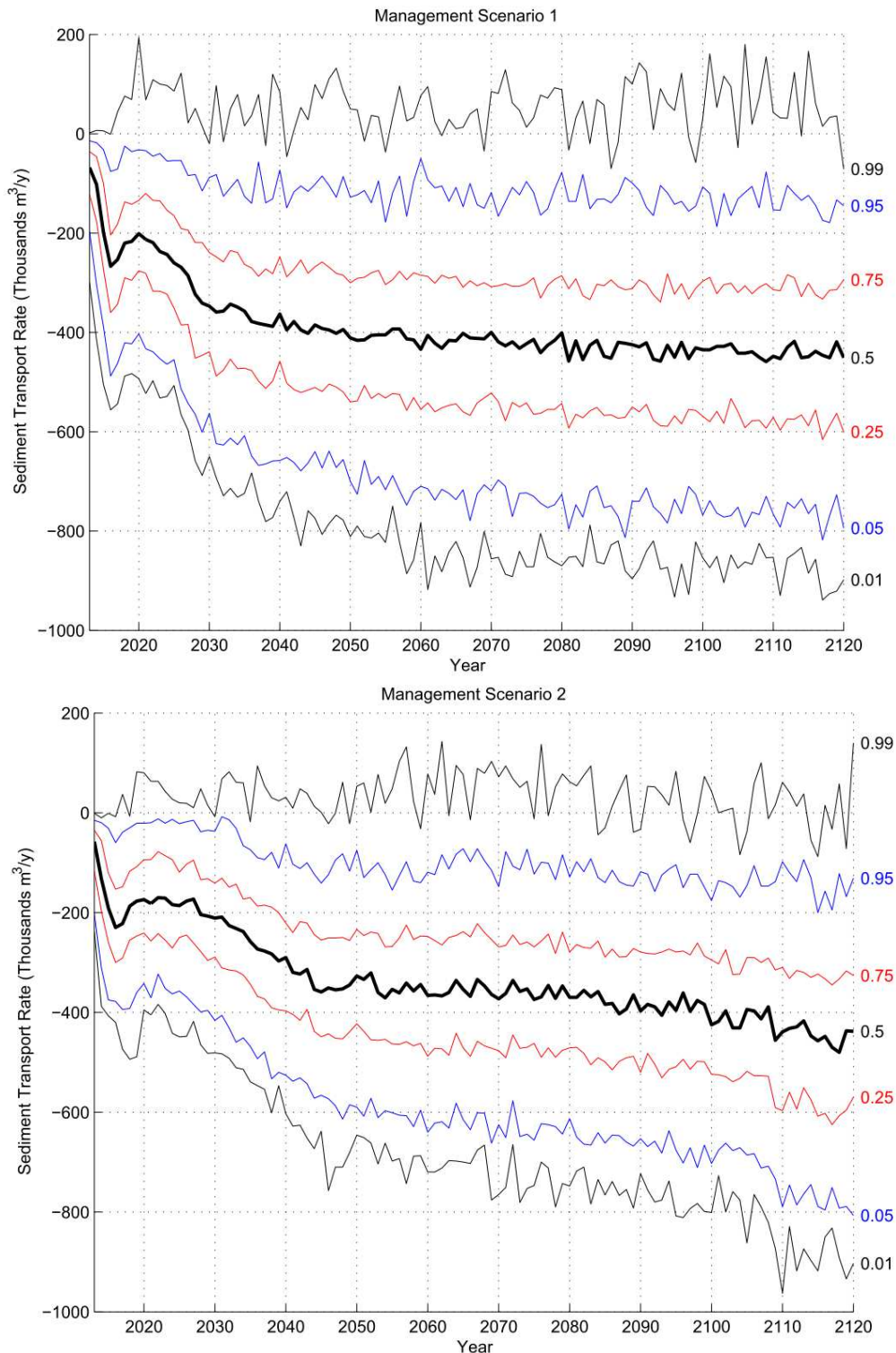
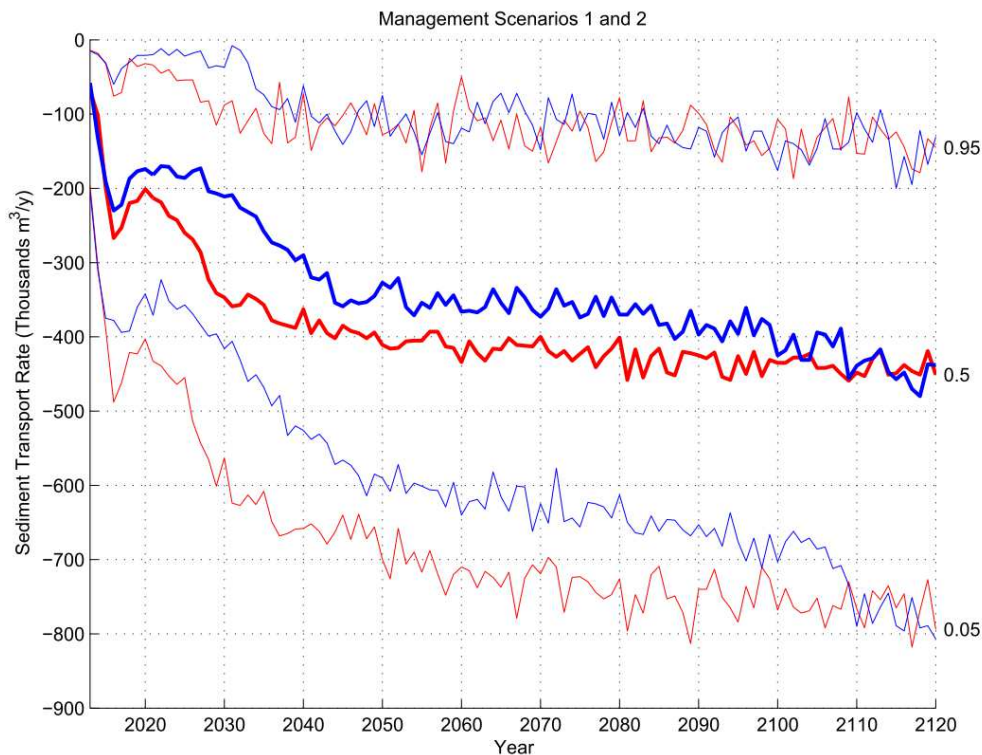


Figure 13. Cliff top recession (as a range) for year 2120; note that the vertical axis represents distance from Winterton Ness (in kilometers), and that the position of various settlements is indicated on the left hand side.



**Figure 14. Average annual sediment transport rates at Cart Gap; positive values indicate transport north; results are shown for Management Scenarios 1 ('Do Nothing', upper image) and 2 ('SMP2 Policy', lower image),**



**Figure 15. Average annual sediment transport rates at Cart Gap; negative values indicate transport south; results are shown for both management scenarios 1 (red lines) and 2 (blue lines).**

For most of the century the transport of sediment to the south is greater under management scenario 1 ('Do Nothing') than under scenario 2 ('SMP2 Policy 6'). This appears to be due to a greater availability of beach sediment, which has been released by the earlier and more widespread failure of coast defence structures. By the end of the century the rates have converged, but there is a clear overall difference in the total volume that passes south from the cliffed frontage. Given that the coast to the south of the cliffed area is artificially nourished, these results imply that less nourishment would be required under a 'Do Nothing' coastal protection policy.

For clarity, the data behind Figure 14 and Figure 15 are also shown in Table 2 and Table 3 (respectively), and have been summarised into decades.



Year	Percentile				
	2.5%	25%	50%	75%	97.5%
2010s	-423	-266	-189	-121	-15
2020s	-519	-353	-259	-167	-11
2030s	-677	-479	-365	-259	-38
2040s	-711	-508	-390	-271	-49
2050s	-748	-531	-407	-288	-73
2060s	-779	-550	-417	-295	-59
2070s	-782	-551	-422	-305	-51
2080s	-800	-566	-432	-308	-44
2090s	-816	-567	-437	-312	-51
2100s	-804	-572	-438	-307	-48
2110s	-820	-581	-441	-310	-65

**Table 2. Average annual sediment transport rates at Cart Gap under Management Scenario 1 ('Do Nothing') for a range of non-exceedance percentiles; thousands of cubic metres per year; negative values indicate transport south.**

Year	Percentile				
	2.5%	25%	50%	75%	97.5%
2010s	-378	-238	-171	-105	-15
2020s	-396	-260	-183	-103	-4
2030s	-498	-343	-250	-167	-15
2040s	-607	-429	-336	-241	-58
2050s	-637	-454	-347	-248	-56
2060s	-663	-472	-356	-247	-37
2070s	-682	-474	-359	-259	-62
2080s	-698	-491	-375	-275	-66
2090s	-721	-507	-387	-279	-54
2100s	-747	-534	-415	-301	-93
2110s	-838	-590	-445	-326	-70

**Table 3. Average annual sediment transport rates at Cart Gap under Management Scenario 2 ('SMP Policy 6') for a range of non-exceedance percentiles; thousands of cubic metres per year; negative values indicate transport south.**

Differences in total sediment transport rate between the two scenarios are summarised in Table 4, per decade, for a range of percentiles. Negative values indicate that Scenario 1 results in a greater transport south.

Year	Percentile				
	2.5%	25%	50%	75%	97.5%
<b>2010s</b>	-45	-27	-18	-16	0
<b>2020s</b>	-123	-94	-76	-64	-8
<b>2030s</b>	-180	-136	-114	-93	-23
<b>2040s</b>	-103	-79	-54	-30	8
<b>2050s</b>	-111	-77	-60	-41	-16
<b>2060s</b>	-116	-78	-60	-48	-22
<b>2070s</b>	-100	-77	-63	-46	11
<b>2080s</b>	-102	-75	-57	-32	22
<b>2090s</b>	-95	-61	-50	-34	2
<b>2100s</b>	-56	-38	-23	-7	45
<b>2110s</b>	19	8	4	16	5

**Table 4. Differences in average annual sediment transport rates at Cart Gap between the two management scenarios (MS1 minus MS2) for a range of non-exceedance percentiles; thousands of cubic metres per year; negative values indicate transport south.**

## 6 INTERPRETATION

Probabilistic SCAPE simulations generate a very large volume of information on the future form of the coast. In this section a small part of this is examined to shed light on some of the workings of the model, and some of the occasionally counter-intuitive insights it provides.

Firstly the projections at Trimingham are examined to explore the relationship between cliff top and toe recession, and the high range of cliff top recession estimated in this area. Secondly the projections at Overstrand are examined to explore why less recession is projected under Management Scenario 1 than under Management Scenario 2 (under which structures are assumed to fail later).

### 6.1 Recession at Trimingham

Close inspection of Figure 10 to Figure 13 reveals that a wide band of cliff top recession is predicted at Trimingham (situated at around 27.5 km on the vertical axis in these figures). In addition very low cliff top recession distances are projected to be possible. Greater detail of this feature of the model output can be seen in Figure 16, which shows the band of projected cliff top recession in this location.

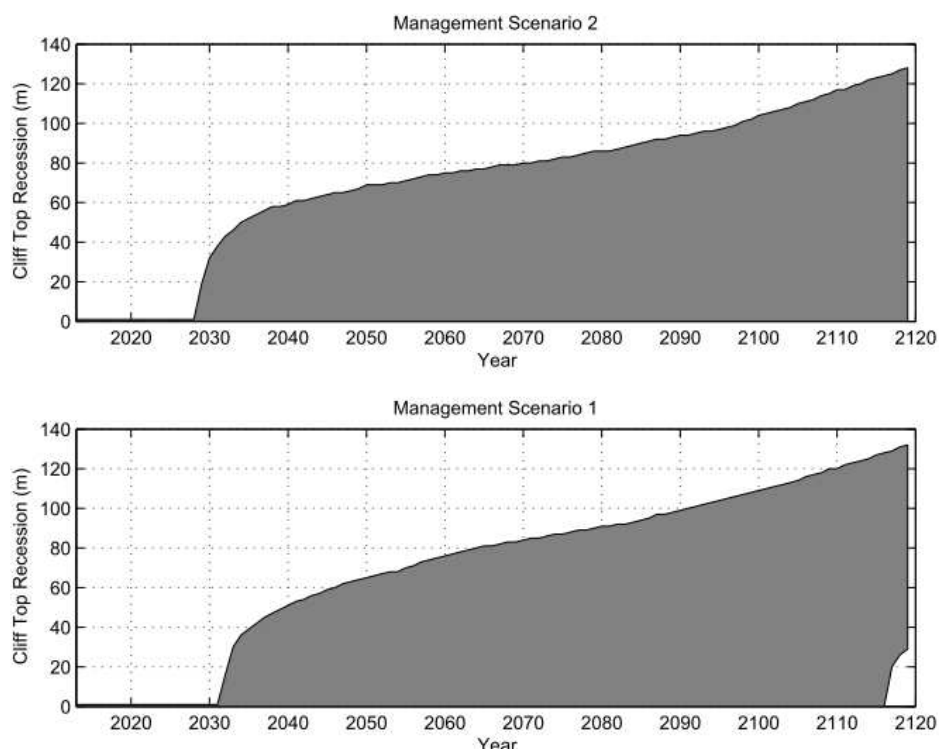


**Figure 16. Cliff top recession at Trimingham (model section 56, 27.5 km from the model origin), the grey areas indicate the range of possible recession distances for any given year.**

The upper limit of projected recession is not particularly high (relative to the rest of the modeled area) but the lower boundary remains at zero for the whole of the simulation period under Management Scenario 2, and only rises above zero at the very end of the

simulation period under Management Scenario 1. In addition, this greater detail reveals that the scenarios show no cliff top recession before approximately 2030 (2031 under Scenario 1, and 2028 under Scenario 2). This is despite the failure of revetment structures at the very start of the simulation and the assumed failure of the local groynes between 2017 and 2022.

The cliff *toe* behavior in this location shows different characteristics, as can be seen in Figure 17.

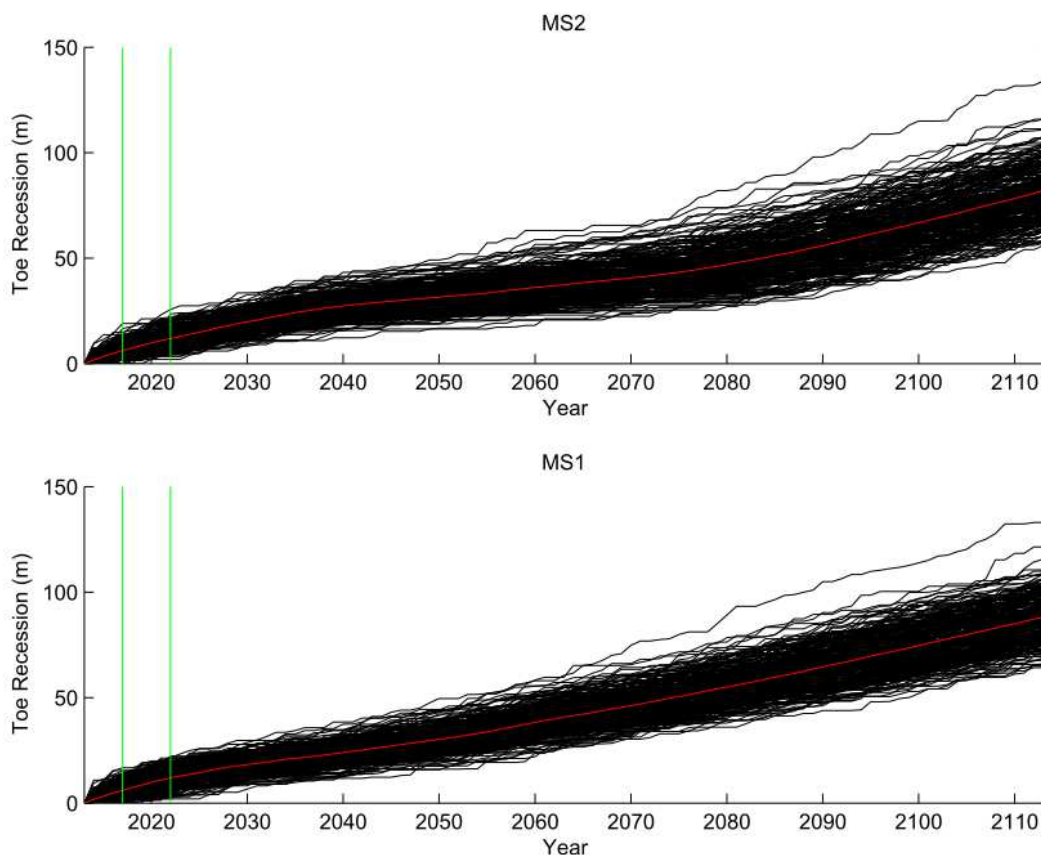


**Figure 17. Projections of cliff *toe* recession at Section 56 (Trimingham); the vertical green lines indicate the range of years in which the local groynes were assumed to fail (the local revetment was assumed to fail at the start of the each simulation and the red line indicates average recession).**

The cliff *toe* recession in this area is continuous throughout the simulation, (i.e. recession does not begin at around 2030, as it does at the cliff top) and is much more closely bounded through the simulation period than the projected possible cliff top recession.

Such behavior seems unrealistic; it implies that: (1) the cliff top is initially unresponsive to cliff *toe* retreat, and (2) that this insensitivity continues throughout the model period for *some* of the simulations.

Investigation revealed that this issue arises in the parameterization of the stochastic land sliding model used to translate SCAPE model projections of the cliff *toe* into cliff top

positions (see Section 3.1). As described above, that model simulates episodic retreat of the cliff top. The size of each episode of recession (i.e. the horizontal retreat distance of the cliff top) depends on the cliff slope *before* and *after* the event, and the height of the cliff (see for example, Figure 5), as described in the equation below.

$$x_i = \frac{h}{\tan \alpha_{fi}} - \frac{h}{\tan \alpha_{si}} \quad \text{Equation 2}$$

Where  $x_i$  represents retreat during event  $i$ ,  $h$  is the cliff height (around 55m in this location) and  $\alpha_{si}$  and  $\alpha_{fi}$  represent the pre and post failure cliff slopes respectively.

$\alpha_{si}$  and  $\alpha_{fi}$  are treated as normally distributed stochastic variables, with the parameters shown in Table 5.

Section	$\alpha_{si}$		$\alpha_{fi}$	
	Mean	Standard deviation	Mean	Standard deviation
	(degrees)	(degrees)	(degrees)	(degrees)
56	30	3	20	5

**Table 5. Cliff failure parameters at model section 56 (Trimingham)**

By combining elements of Table 5 within Equation 2 an estimate can be made of the maximum horizontal recession distance between failure events in this area, as follows:

$$x_{i\_max} = \frac{55}{\tan(20 - 1.96 \times 5)} - \frac{55}{\tan(30 + 1.96 \times 3)}$$

or

$$x_{i\_max} = 230m$$

This implies that the cliff toe *may* retreat by as much as 230 metres between cliff top failure events. This is an estimate of a maxima, but it follows that the general scale of  $x_i$  is large.

The realism of this representation depends quite strongly on the parameters in Table 5. These were estimated by a national expert (within the British Geological Survey) but such parameters are inherently difficult to establish and unavoidably subjective, to a degree.

The lack of cliff top recession during the early years, and the projection of (possible) zero recession in this area throughout the next century, arises for a related reason. As described in Section 3.1, each simulation begins with a stochastic estimate of an *initial* cliff slope. In this location that initial slope was estimated to be 35 degrees (as a mean, with a standard deviation of 3 degrees). This is very steep relative to  $\alpha_{si}$  meaning that a cliff failure (and therefore cliff top retreat) is *highly likely* at this location in the early stages of the simulation. This occurs in the simulations (which begin in the year 2000),

but because the results are related to cliff position in 2012, this early retreat is filtered out of the results i.e. the model simulates this cliff failure prior to 2012. No cliff top recession is then seen before (approximately) 2030 (as shown in Figure 16) because of the generally large scale of  $x_i$  (as described above).

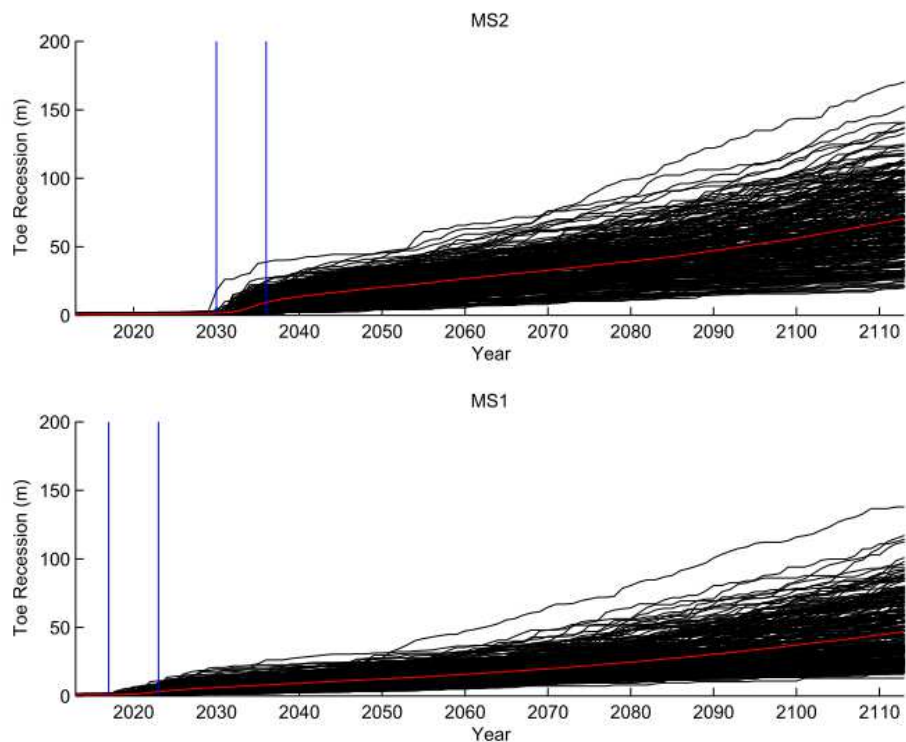
The key implication for the project is that the projected absence of recession of the cliff top before around 2030 at Trimmingham should be considered to be unreliable. The process of expert interpretation that should be applied to such modeling should pay particular attention to this location with a view to substituting an alternative (non-zero) retreat rate in this location, in the early decades. The cliff toe recession shown in Figure 17 could be used to inform this process.

The wide bands of recession (i.e. the possibility of very low cliff top recession at Trimmingham throughout the next century) should also be interpreted with caution. This reflects real uncertainty (in conditions of cliff stability) but is also partly an artifact of the process of normalizing model output to the cliff position in 2013.

## 6.2 Recession at Overstrand

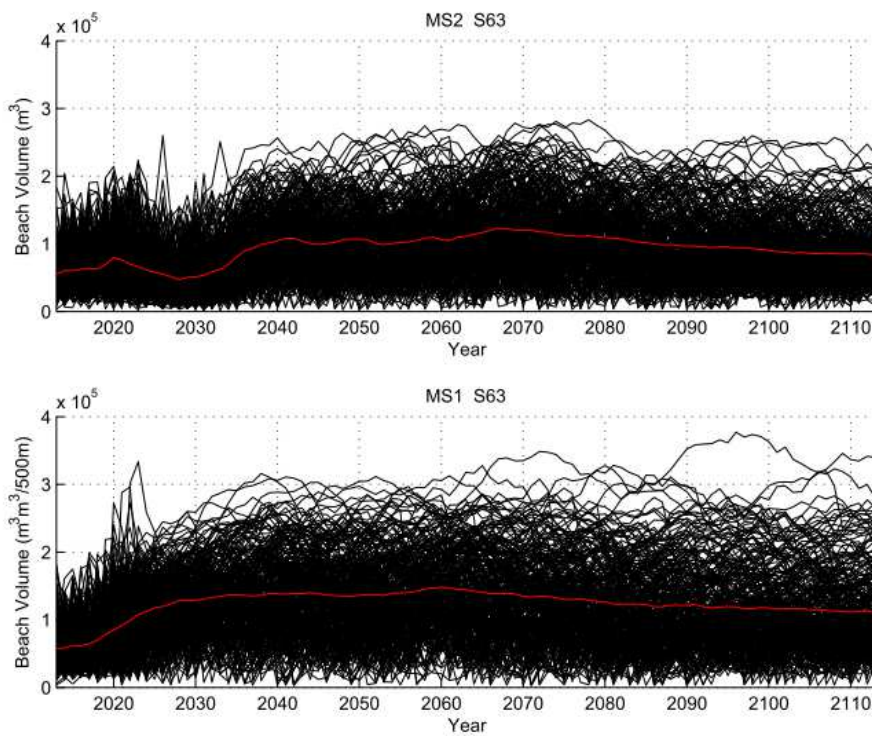
Close inspection of the recession projections reveals the surprising result that a 'Do Nothing' policy at Overstrand, in which defences are abandoned, results in less cliff top recession than the 'SMP2' policy, under which seawalls and some revetments are maintained for longer. The reason for this is explored below, by examining model output at model section 63, which passes through Overstrand.

Figure 18 shows the recession in this location under all the (2 x 250) simulations. It illustrates the fact that cliff toe recession at Section 63 is less under the 'Do Nothing', policy (bottom image), despite the earlier failure of coast protection structures in this area (the dates of which are indicated by the vertical blue lines).



**Figure 18. Cliff toe recession at Section 63 (2x250 simulations, averages are shown in red), under policies ‘SMP2’ (upper panel) and ‘Do Nothing’ (lower panel); vertical blue lines indicate the period during which the coast protection structure at this point along the coast (a revetment) is assumed to fail.**

Although the structures fail earlier under the ‘Do Nothing’ scenario, local beach volumes drive down the subsequent trajectories of recession, as shown in Figure 13.



**Figure 19. Beach volume across Section 63 (2 x 250 simulations, averages are shown in red)**

This is due to the volume of the beach, which plays an important role in protecting cliffs and shore platforms; larger beaches provide more protection.

When the beach volumes at Section 63 (S63) are plotted (in Figure 19), it can be seen that the beach is fuller under the 'Do Nothing' scenario (Management Scenario 1, lower image). The large number of simulations complicate the comparison between the two scenarios, and so average beach volumes are shown in Figure 20, along with the average recession of this section.



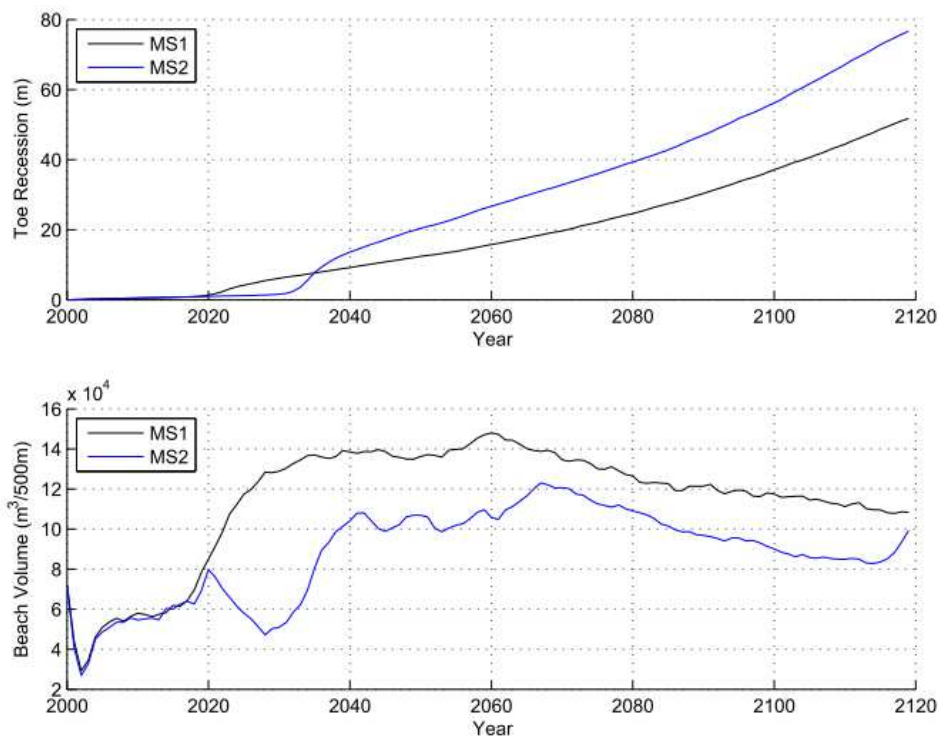


**Figure 20. Average beach volumes (lower panel) and toe recession distances (upper panel) across Section 63 under the ‘Do Nothing’ scenario (black lines) and ‘SMP2 Policy 6’ (blue lines).**

It can be seen that under the ‘Do Nothing’ scenario (MS1) the beach is substantially larger from 2020 onwards, and that these larger beaches are associated with lower recession rates.

This larger beach is due to it being bulked by sediment released from the cliffs and shore platform. The release of such sediment from Section 63 is shown in Figure 21.

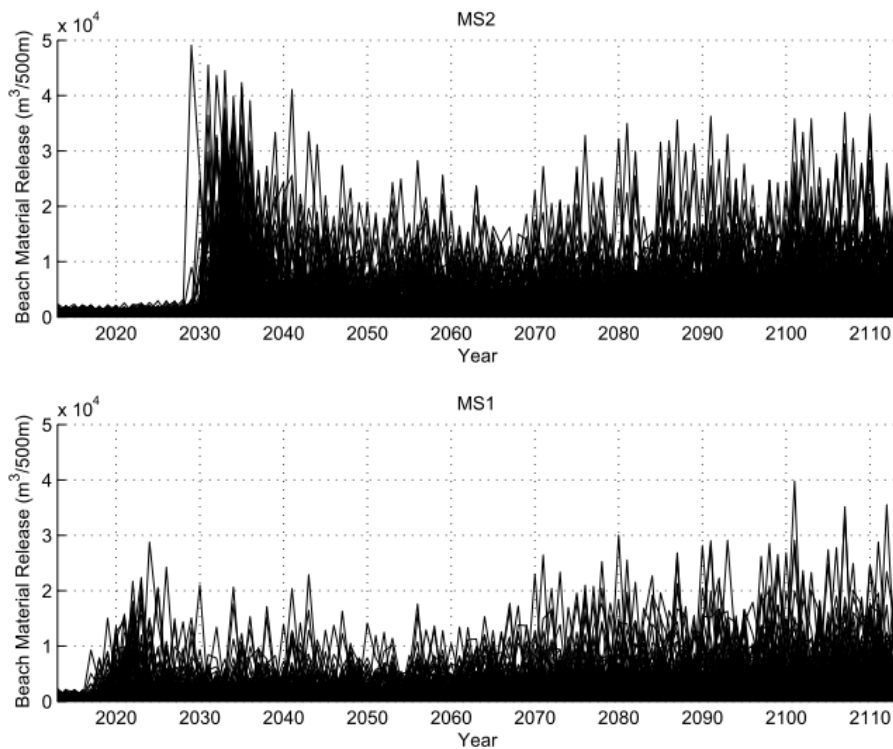


**Figure 21. Volumes of sediment release from the cliff and shore platform across Section 63 under the ‘Do Nothing’ scenario (lower panel) and ‘SMP2 Policy 6’ scenario (upper panel): (2x250 simulations.**

The averages of these simulations are shown in Figure 22.

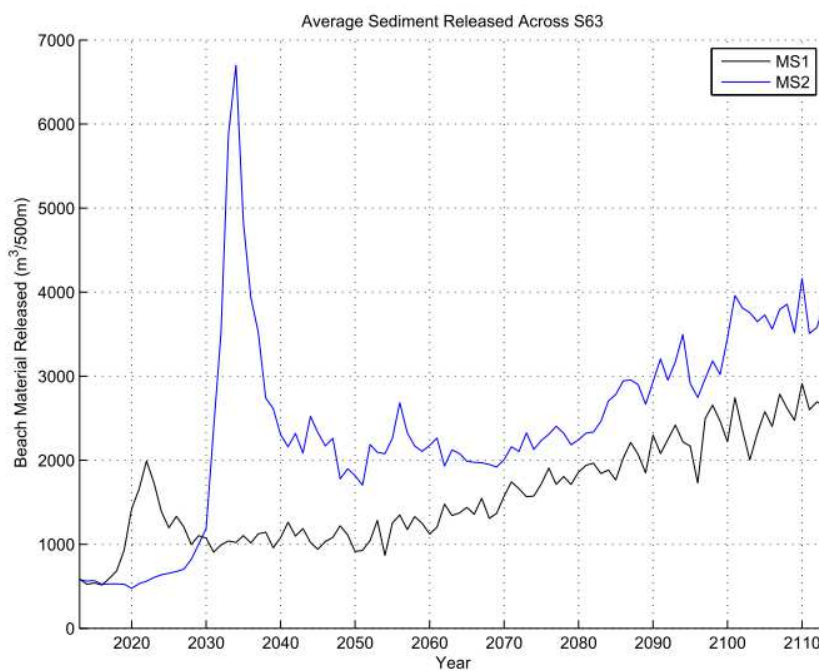


**Figure 22. Average volumes of sediment release from cliff and platform across Section 63 under the ‘Do Nothing’ scenario (black line) and the ‘SMP2’ scenario (blue line).**

It can be seen that the 'Do Nothing' policy results in less sediment being released from Section 63 (because the cliff recession is less), but the release begins at an earlier date. Clearly this pattern of release does not explain the greater beach volumes that occur here under the 'Do Nothing' scenario.

Much of the beach sediment at Section 63 comes from cliff and platform erosion to the west (i.e. towards Cromer). The sediment released from the (4.5 km) study area towards the west of Section 63 is shown in Figure 23.

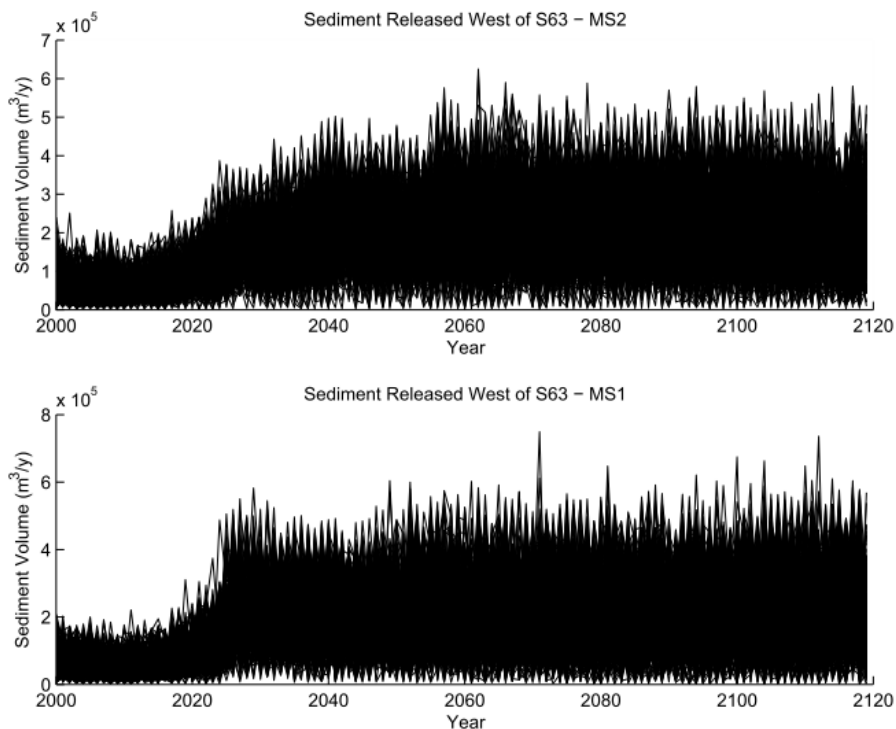


**Figure 23. Volumes of sediment release from cliff and platform west of Section 63 (2x250 simulations)**

The averages of these simulations are shown in Figure 24.

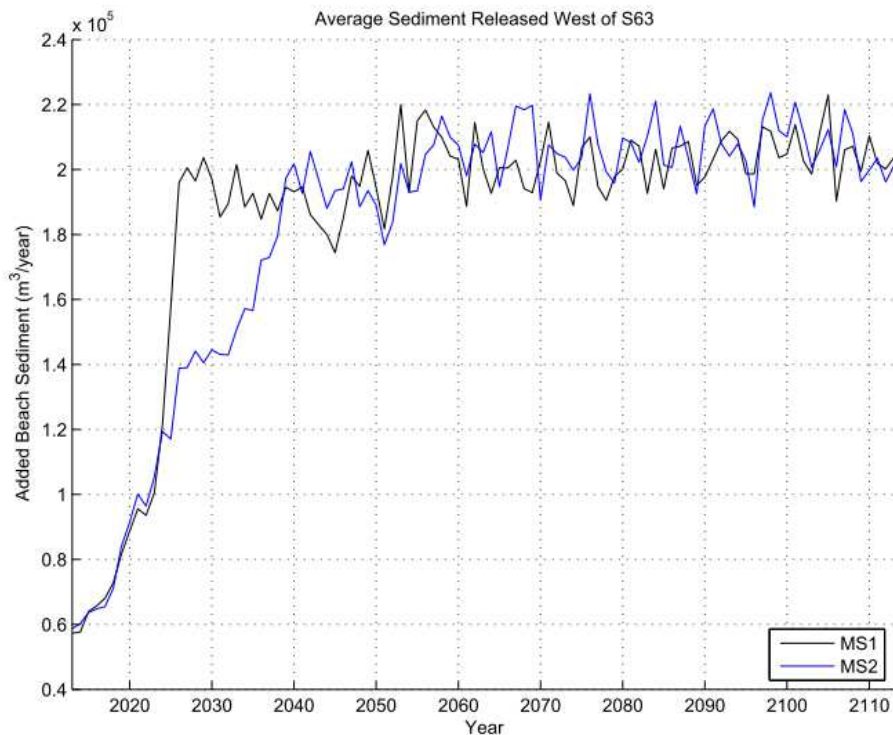


**Figure 24. Average volumes of sediment release from cliffs and platforms west of Section 63**

It is clear that more sediment is released from the section of coast towards (and at) Cromer under the 'Do Nothing' scenario (MS1). This material then is transported southwards, and this explains why the beaches at S63 are larger, and why the recession there is lower (under MS1).

The data in Figure 24 represent annual rates of sediment release. The *difference* in sediment release between the 'Do Nothing' and 'SMP2' policies is shown in Figure 25.

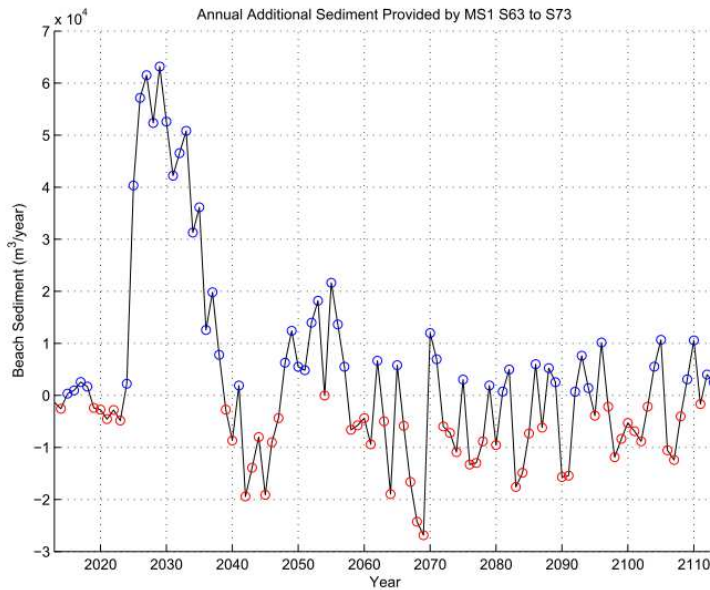


**Figure 25. Additional volumes of sediment release from cliff and platform due to the ‘Do Nothing’ scenario 1 (for the study cliffs west of Section 63; positive indicates more sediment release under this scenario).**

It can be seen that, at its peak, around 60,000 m<sup>3</sup> of *additional* sediment is released in this area per year under the ‘Do Nothing’ scenario. Figure 26 integrates this difference through time, to provide the total difference in released beach volume.

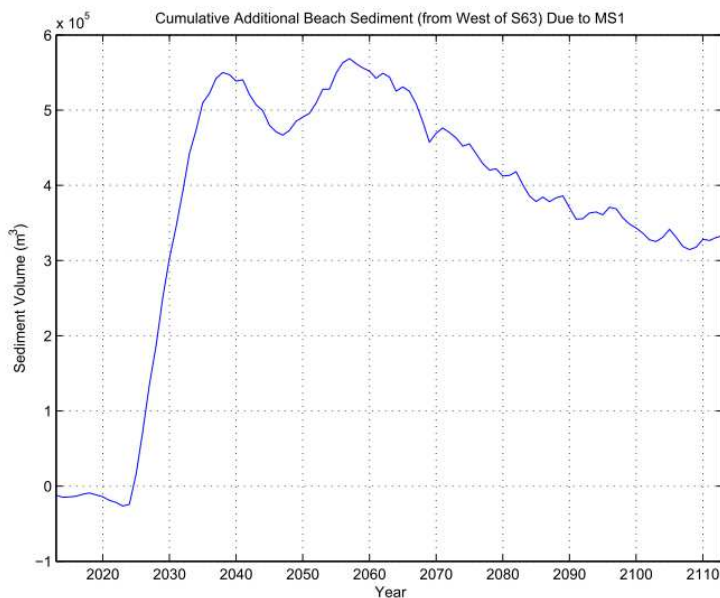


**Figure 26. Cumulative additional volumes of sediment release from cliff and platform due to the ‘Do Nothing’ scenario 1 (west of Section 63 to Cromer)**

Figure 26 shows that, at its peak (in the 2050s) more than 0.5 million cubic metres of additional sediment has been released west of Section 63.

## 7 SUMMARY

The Soft Cliff And Platform Erosion (SCAPE) modelling tool has, under previous studies, been used to represent the Norfolk coast between Blakeney Spit and Winterton Ness. In this study it is used to explore the consequences of two alternative strategies of future coastal management, 'Do Nothing' and 'SMP2 Policy'. These strategies are implemented in the model through representation of the estimated years of failure of the existing coast protection structures (which were provided by Mott MacDonald staff). These years are represented in the probabilistic terms of lower and upper limits of possible failure year.

The models were then run probabilistically (250 simulations per scenario) and used to estimate the upper and lower limit of cliff top position every year to 2120. In addition the annual sediment flux at the southern limit of the cliffs was recorded.

These results were then passed to Mott MacDonald to be used to assess the relative merits of the management strategies (see Appendix C). This should include a process of interpretation by experts with good knowledge of local conditions and the history of coastal change across the study area. This process should, in particular, include consideration of revision of the low recession rates projected at Trimingham.

Inspection of the models revealed how the release of sediment following structure failure can provide positive benefit in downdrift terms, both in terms of reduced erosion in some areas (even when structures here have failed at an earlier date) and, a reduced need to artificially nourish the beaches south of Cart Gap.

### References

Chang S-C, Evans G (1992) Source of sediment and sediment transport on the east coast of England: significant or coincidental phenomena? *Mar Geol* 107:283 – 288

Clayton KM (1989) Sediment input from the Norfolk Cliffs, Eastern England – a century of coast protection and its effect. *J Coast Res* 5:433 – 442

Dawson, R., Dickson, M., Nicholls, R., Hall, J., Walkden, M., Stansby, P., Mokrech, M., Richards, J., Zhou, J., Milligan, J., Jordan, A., Pearson, S., Rees, S., Bates, P., Koukoulas, S., Watkinson, A., (2009) Integrated analysis of risks of coastal flooding and cliff erosion under scenarios of long term change. *Climatic Change*, *Climatic Change* (2009) 95:249-288. DOI 10.1007/s10584-008-9532-8. Springer.

Dickson, M.E., Walkden, M.J.A. and Hall, J.W., 2007. Systemic impacts of climate change on an eroding coastal region over the twenty-first century. *Climatic Change*, 84(2): 141-166.

Environment Agency (2011) Environment Agency 2011 Adapting to Climate Change: Advice for Flood and Coastal Erosion Risk Management Authorities.

Environment Agency 2006. Flood and Coastal Defence Appraisal Guidance FCDPAG3 Economic Appraisal Supplementary Note to Operating Authorities – Climate Change Impacts

Hanson, H., 1989. GENESIS: Generalised Model for Simulating Shoreline Change: Report 1, Technical Reference. Technical Report, CERC-89-19.

Hall JW, Lee EM, Meadowcroft IC (2000) Risk-based benefit assessment of coastal cliff protection. Proc Inst Civ Eng Water Marit Eng 142:127–139, Sept

Kamphuis, J., 1987. Recession rates of glacial till bluffs. Journal of Waterway, Port, Coastal, and Ocean Engineering 113 (1), 60–73.

Lee EM, Clark AR (2002) Investigation and management of soft rock cliffs. Thomas Telford, London

Nairn, R.B. and Southgate, H.N., 1993. Deterministic profile modelling of near-shore processes. Part 2. Sediment transport and beach profile development. Coastal Engineering, 19, 57–96.

North Norfolk District Council (2004) Overstrand to Walcott Strategy Study.

Pelnard-Considere R (1956) Essai de theorie de l' evolution des forms de ravage en plage de sable et de galets. 4th Journees de l' Hydraulique, Les Energies de la Mer Question III:792 – 808

Skafel, M.G., 1995. Laboratory measurement of nearshore velocities and erosion of cohesive sediment (Till) shorelines. Technical note. Coastal Engineering 24, 343–349.

University of Bristol (2002) for HR Wallingford and North Norfolk District Council SCAPE modelling of the Norfolk Coast, report for the Overstrand to Walcott Strategy Study.

Vincent CE (1979) Longshore sand transport rates – a simple model for the East Anglian coastline. Coast Eng 3:113 – 136

Walkden, M.J.A. and Hall, J.W., 2005. A predictive Mesoscale model of the erosion and profile development of soft rock shores. Coastal Engineering, 52(6): 535-563.

Walkden, M. J., and Hall, J. (2011) A Mesoscale Predictive Model of the Evolution and Management of a Soft-Rock Coast Journal of Coastal Research 27 3 529–543 May.